C and S induce changes in the electronic and geometric structure of Pd(533) and Pd(320)

2006 J. Phys.: Condens. Matter 18 8015

(http://iopscience.iop.org/0953-8984/18/34/013)

INSTITUTE OF PHYSICS PUBLISHING JOURNAL OF PHYSICS: CONDENSED MATTER

J. Phys.: Condens. Matter **18** (2006) 8015–8027 doi:10.1088/0953-8984/18/34/013

C and S induce changes in the electronic and geometric structure of Pd(533) and Pd(320)

Faisal Mehmood, Sergey Stolbov and Talat S Rahman

116 Cardwell Hall, Department of Physics, Kansas State University, Manhattan, KS 66506-2600, USA

Received 21 June 2006, in final form 24 July 2006
Published 11 August 2006
Online at stacks.iop.org/JPhysCM/18/8015

Abstract

We have performed *ab initio* electronic structure calculations of C and S adsorption on two vicinal surfaces of Pd with different terrace geometries and widths. We find that both adsorbates induce a significant perturbation of the surface electronic and geometric structure of Pd(533) and Pd(320). In particular, C adsorbed at the bridge site at the edge of a Pd chain in Pd(320) is found to penetrate the surface to form a sub-surface structure. The adsorption energies show an almost linear dependence on the number of adsorbate–metal bonds, and lie in the ranges 5.31–8.58 eV for C and 2.89–5.40 eV for S. A strong hybridization between adsorbate and surface electronic states causes a large splitting of the bands, leading to a drastic decrease in the local densities of electronic states at the Fermi level for Pd surface atoms neighbouring the adsorbate, which may poison catalytic activity of the surface. Comparison of the results for Pd(533) with those obtained earlier for Pd(211) suggests a local character of the impact of the adsorbate on the geometric and electronic structures of Pd surfaces.

(Some figures in this article are in colour only in the electronic version)

1. Introduction

The elementary processes in heterogeneous catalysis, such as the adsorption of reactants and their diffusion and reaction, are caused by the formation, modification or breaking of chemical bonds between the molecules and a catalyst. Since the nature of the chemical bonds is determined by the interplay of the electronic and geometric structures of the catalyst surface, these characteristics are the focus of numerous studies.

Real catalysts usually have a complex geometric structure, because they are highly dispersed as small particles on substrates. The surface of these particles may have microfacets with high Miller index planes consisting of steps and kinks which may influence the reactivity of catalyst surfaces significantly [1–8]. For instance, the N_2 association reaction is extremely sensitive to the presence of steps. For Ru(0001), its rate at the step edges is found experimentally to be at least nine orders of magnitude higher than that on its terrace, at

500 K [3]. The sticking coefficient of O_2 on the stepped surface, Ag(410), is also found to be higher than that on Ag(100), as measured in a recent high-resolution electron energy loss (HREEL) spectroscopy experiments [9].

The specific role of step atoms in a chemical reaction may, however, be more complex and may not always lead to enhanced reactivity. Experimental observations do not show any effect of steps on the rate of CO oxidation on Pt(335) [10] or other metal surfaces [11]. The results of first-principles calculations for the reactions on Pd(211), Pd(311) [6] and Ir(211) [11] also indicate that CO oxidation barriers are insensitive to the local surface geometry. It has also been pointed out [12] that dissociation reactions are always structure-sensitive (surface steps are favoured for the reactions), while association reactions may not always be so. Furthermore, the reactions with a high valence reactant are usually more structure-sensitive.

Apart from steps and kinks, there are other imperfections that may affect surface reactivity. In real catalytic processes, some sub-products of reactions or other gases present in the reaction environment may atomically adsorb on the catalyst surface and change its reactivity. For instance, sulfur-containing molecules are common impurities in gasoline. During CO catalytic oxidation in car exhaust refinement systems, sulfur, which is known to be an inhibitor for many catalytic reactions, adsorbs atomically on the catalyst surface and poisons the surface reactivity. In one of the earlier studies [13], it was suggested that the depletion of the local density of states (LDOS) at the Fermi level [$N_a(E_F)$] (where a denotes the atom contributing to the LDOS) upon S adsorption can cause poisoning of the surface reactivity. Computational studies of S adsorption on some Pd surfaces [14–16] also show a reduction of $N_a(E_F)$ due to a strong hybridization of the p states of S with the d states of Pd. Several experimental studies also focus on the poisoning effect of S on metal surfaces [17–19]. Although the rate of CO dissociation during catalytic oxidation is low, a small amount of C can atomically adsorb on the catalyst surface. Our recent results [14, 15] show that C atoms adsorbed on Pd stepped surfaces suppress substantially the $N_a(E_F)$ of the neighbouring surface atoms, which may be taken as an indication of poisoning. Atomic carbon adsorption on a Pd surface and its poisoning effect have also been reported for the case of catalytic vinyl acetate synthesis [20]. Moreover, since step sites are generally more reactive than others on the terrace, they are also prone to attract more impurities. The combination of steps and atomically adsorbed impurities may thus have a significant impact on the reactivity of catalysts.

Motivated by the above, we have investigated the effect of C and S adsorption on the geometric and electronic structures of Pd(533), a vicinal of Pd(111), and compared them with that on Pd(320), a vicinal of Pd(110), for several reasons. First, a comparative study of the effect of C and S on a stepped transition metal surface would provide a measure of the strength of the impurity substrate bond and its impact on the surface electronic structure. Second, as the atoms along the steps of Pd(533) and Pd(320) have local coordinations of 7 and 6, respectively, a systematic study of C and S adsorption on these two surfaces is a step towards understanding the role of undercoordinated sites in chemical reactivity. Third, comparison of the results on Pd(533) with those already available for Pd(211), a smaller terrace but of similar geometry, will provide insights on the role of the terrace width on the chemisorption process. Finally, examination of the relative effect of C and S on Pd(320) will provide the basis for comparison of results on stepped surfaces with fcc(110) terrace geometry to those with fcc(111) terraces [14]. Since the nonequivalent atoms on a vicinal surface, in the presence of an adsorbate, account for a complex and inhomogeneous system, these studies are expected to have implications also for the characteristics of nanoparticles that contain a range of undercoordinated sites in complex environments. Note that, in an earlier study, Makkonen *et al* [15] have already presented some results for the energetics of S adsorption on Pd(320). We have repeated these calculations and included the results here only for completeness.

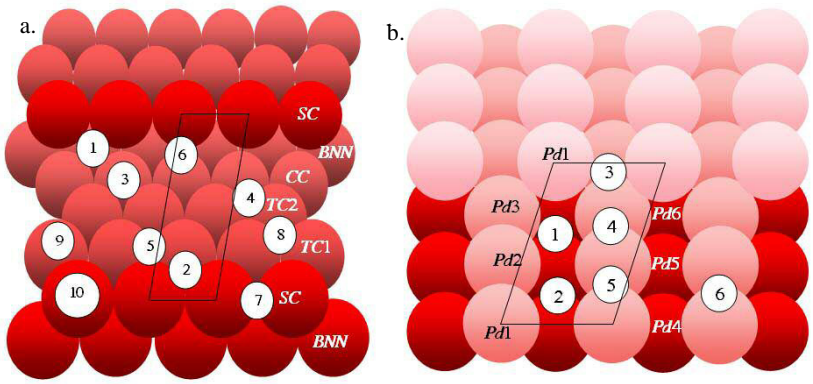

Figure 1. Adsorption sites on (a) Pd(533) and (b) Pd(320).

2. Details of computational method

The present first-principles calculations are based on density functional theory (DFT) [21] with the generalized gradient approximation (GGA) [22] for the exchange–correlation potential. Optimized surface structures and the adsorption energies (E_{ad}) have been calculated using the plane wave pseudopotential method (PWPP) [23] with ultrasoft pseudopotentials [24], while the full potential linearized augmented plane wave (FLAPW) method [25], as embodied in the WIEN2K code [26], has been used to calculate the detailed electronic structure including the LDOS and valence charge densities for the most interesting systems.

The fcc(533) surface consists of a four-atom-wide (111) terrace and a monatomic (100) micro-facetted step edge. A perspective view of such a surface is shown in figure 1(a). Throughout this paper we have used the following nomenclature to describe the chains of atoms on this surface: SC (step chain), consisting of the step edge atoms; TC1 (terrace chain 1) for the chain passing through terrace atoms next to the step edge; TC2 (terrace chain 2) for the chain through the terrace atoms adjacent to the corner atoms; CC (corner chain) for the chain located between TC2 and SC; and BNN (bulk nearest neighbour) for those located just beneath SC. The Pd(533) surface was modelled by a supercell consisting of a 22-layer slab and 12 Å of vacuum.

The Pd(320) is a stepped surface with three-atom-wide (110) terraces and a monatomic (100) micro-facetted step edge. Because the fcc(110) geometry is more open than the close-packed fcc(111), a kinked structure is formed along the step edge in Pd(320) (see figure 1(b)). For this surface, we have used notations Pd1, Pd2, Pd3, and so on, to describe corresponding atoms in different layers of the surface. The Pd(320) supercell included a 19-layer slab and 11 Å of vacuum. The surfaces adsorbed with S or C contained one adsorbate atom per primitive two-dimensional unit cell, shown in figure 1. This corresponds to adsorbate coverage of 1/4 monolayer (ML) for Pd(533) and 1/3 ML for Pd(320).

For all PWPP calculations we used an energy cut-off of 290 eV, which was found to be sufficient. A Monkhorst–Pack k-point mesh [27] of $(10\times10\times10)$, $(10\times3\times1)$ and $(10\times4\times1)$ was used to model bulk Pd, Pd(533) and Pd(320), respectively. The bulk lattice constant was calculated to be 3.96 Å, which is almost 2% higher than the experimental value [28] and is typical of results obtained from DFT/GGA. During the lattice relaxations, all atoms were allowed to fully relax in all directions until forces on each atom were less than 0.02 eV $Å^{-1}$.

For the most interesting structures, the relaxed geometries obtained from PWPP calculations were used as input for the WIEN2K code, which further refined the geometries in a

Table 1. Multilayer relaxation for Pd(533).

$\delta\mathbf{d}_{i,i+1}$	S/Pd(533)	C/Pd(533)	Pd(533)
$\delta\mathbf{d}_{1,2}$	−12.3	+29.7	−15.8
$\delta\mathbf{d}_{2,3}$	−19.7	+3.7	−11.9
$\delta\mathbf{d}_{3,4}$	+44.7	−32.0	−6.6
$\delta\mathbf{d}_{4,5}$	−4.2	+36.0	+24.3
$\delta\mathbf{d}_{5,6}$	−22.5	+3.4	−6.8
$\delta\mathbf{d}_{6,7}$	+5.9	−8.4	−10.1
$\delta\mathbf{d}_{7,8}$	+14.3	+3.6	+5.8
$\delta\mathbf{d}_{8,9}$	−4.1	+7.2	+4.1
$\delta\mathbf{d}_{9,10}$	−14.4	−5.1	−6.7
$\delta\mathbf{d}_{10,11}$	+9.4	−4.2	−0.2

few ionic iterations. In the FLAPW method, the LDOS and local charges are calculated through integration over muffin-tin (MT) spheres of radius R_{MT}. To analyse the effect of the adsorbate on these specific quantities, the set of R_{MT} for Pd atoms should be chosen to be the same for both the clean and the adsorbate-covered surface. Ideally, R_{MT} should be as large as possible without causing the MT spheres to overlap. For bulk Pd atoms, a choice of $R_{\mathrm{MT}} = 1.38$ Å was found to be optimal. However, for the Pd atoms with direct bonds to C and S, $R_{\mathrm{MT}} = 1.08$ Å (for C) and $R_{\mathrm{MT}} = 1.22$ Å (for S) provided more compatibility with the shorter C–Pd and S–Pd bond lengths. For C atoms $R_{\mathrm{MT}} = 0.926$ Å, and for S atoms $R_{\mathrm{MT}} = 1.08$ Å was found to be appropriate. In order to include a reasonably large number of plane waves ($RK_{\max} = 7$) with the reduced R_{MT} s for the surface atoms, we used basis sets of 1678, 3039 and 4795 LAPWs for Pd(533), S/Pd(533) and C/Pd(533), respectively. The calculations were performed for the $(10 \times 3 \times 1)$ and $(6 \times 3 \times 1)$ k-point mesh in the Brillouin zone for Pd(533) and Pd(320), respectively.

3. Results and discussion

3.1. Surface relaxations

Optimized geometric structures of Pd(533) and Pd(320) with adsorbed S and C were obtained for ten possible adsorption sites on the former and six sites on the latter, as shown in figure 1. We find the adsorbate to perturb the structures of both surfaces substantially, regardless of which site it takes. For Pd(533), the effect is found to be most dramatic if S or C adsorb on site # 1, as labelled in figure 1. Surface lattice relaxation is usually characterized by changes in the interlayer separations $\delta\mathbf{d}_{i,i+1}$, which are defined as the distances between neighbouring surface planes. In table 1, we show deviations of $\delta\mathbf{d}_{i,i+1}$ from those obtained for the bulk terminated surface. In the case of clean Pd(533), these deviations characterize the relaxation introduced upon creation of the surface from bulk material, while for Pd(533) with adsorbed S or C, the presence of the adsorbate also affects the nature of the surface relaxation. As seen from table 1, S and C perturb the surface relaxation pattern of Pd(533) in very different manners. This is caused by differences in the adsorption geometries of S and C illustrated in figure 2. During the relaxation, the smaller size of the C atom allows it to penetrate the surface and form chemical bonds with the CC, SC and BNN atoms. To keep the optimal C–Pd bond lengths, the separation between SC (layer 1) and BNN (layer 5) atoms is expanded, causing an increase in $\delta\mathbf{d}_{1,2}$ and $\delta\mathbf{d}_{4,5}$. In contrast, the relatively larger size of the S atoms keeps them outside the step corner. They form bonds with SC and CC atoms and build extra S–TC2 bonds

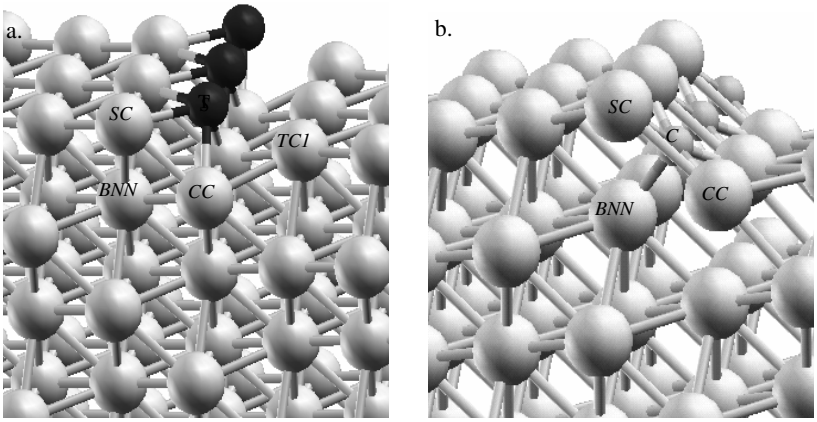

Figure 2. Relaxed geometric structure of (a) $S_{0.25}$/Pd(533) and (b) $C_{0.25}$/Pd(533) shows the difference in bonding for S and C.

Table 2. Multilayer relaxation for Pd(320).

$\delta\mathbf{d}_{i,i+1}$	S1/Pd(320)	C1/Pd(320)	C5/Pd(320)	Pd(320)
$\delta\mathbf{d}_{1,2}$	−24.4	+26.4	+38.1	−15.4
$\delta\mathbf{d}_{2,3}$	−5.5	−55.7	+1.0	−18.7
$\delta\mathbf{d}_{3,4}$	−8.3	+45.5	−0.8	+1.4
$\delta\mathbf{d}_{4,5}$	+34.9	−8.5	+4.1	−10.1
$\delta\mathbf{d}_{5,6}$	−16.4	+23.9	−5.6	+21.3
$\delta\mathbf{d}_{6,7}$	−3.2	−9.6	+16.5	−7.0
$\delta\mathbf{d}_{7,8}$	+12.4	+9.6	−3.6	−1.7
$\delta\mathbf{d}_{8,9}$	−14.1	−4.8	+7.9	+2.4
$\delta\mathbf{d}_{9,10}$	+11.5	+0.8	−4.4	−1.4

which induce upward displacement of the TC2 atoms (layer 3) and hence an increase in $\delta\mathbf{d}_{3,4}$. Interestingly, our recent calculations performed for Pd(211) reveal a similar response of the surface lattice to S and C adsorption [14]: the separation between SC and BNN is substantially increased upon C adsorption and TC is displaced upwards upon S adsorption. Note that Pd(211) has one less chain of atoms on its terrace compared to that of Pd(533). This similarity reflects the predominantly local character of the perturbation induced by the adsorbate. The surface atoms are displaced to form chemical bonds with the adsorbate affecting mostly the nearest neighbours. However, some difference in the magnitudes of atomic displacements found for Pd(533) and Pd(211) may be traced to long-range interactions. It should be mentioned that the surfaces under consideration are high Miller index surfaces with small interlayer separations (for Pd(533) it is only 0.604 Å). Therefore the large percentage of interlayer separation shown in table 1 corresponds to less dramatic absolute shifts. Nevertheless, $\delta\mathbf{d}_{3,4} = +44.7\%$ obtained for S/Pd(533) is 0.27 Å, or 9% of the Pd–Pd bond length, which is a significant factor and reflective of strong perturbation induced by the adsorbate.

Lattice relaxation upon S and C adsorption has also been studied for the kinked Pd(320) surface. The results for $\delta\mathbf{d}_{i,i+1}$ for S and C adsorbed at site 1 (figure 1) are shown in table 2. In general, the calculated relaxation pattern $(- - + - +)$ for clean Pd(320) matches well with low-energy electron diffraction (LEED) results [29]. As in the case of Pd(533), the size and chemical composition of the adsorbate atom have a remarkable effect on the relaxation patterns for S/Pd(320) and C/Pd(320), which are strikingly different. C atoms penetrate the

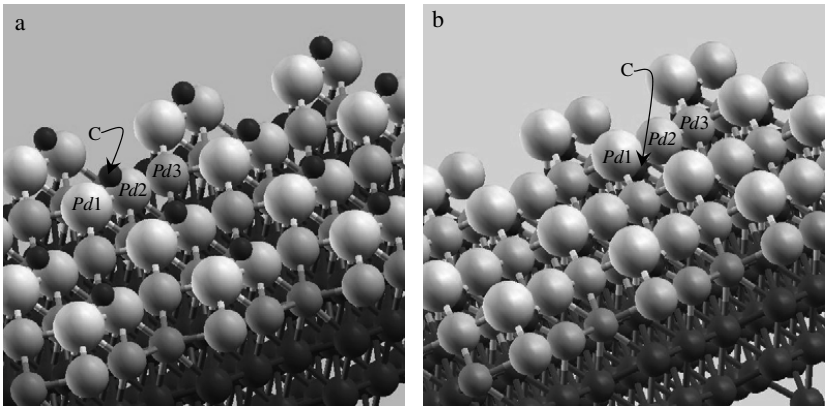

Figure 3. (a) Initial and (b) final relaxed geometric structures of $C_{0.33}$/Pd(320) on site 5.

Table 3. C and S adsorption energies at various sites on Pd(533) and Pd(320).

Site	S/Pd(533)	C/Pd(533)	C/Pd(320)
1	5.40	8.44	8.58
2	5.31	7.52	8.29
3	5.28	7.49	8.47
4	5.28	7.49	7.30
5	5.26	7.43	8.49
6	5.09	7.10	5.53
7	4.62	6.32	
8	4.72	5.85	
9	4.25	5.58	
10	4.13	5.31	

kink site and form bonds with five neighbouring surface atoms, including Pd1, two Pd3, Pd5 and Pd6. Optimization of bond length causes the displacements of all these atoms, giving rise to a significant multilayer relaxation. The S atoms, on the other hand, stay above the kink site and cause a substantial displacement only for Pd1 and Pd5 atoms. Also for the case of S on Pd(320), the surface relaxations reported here are in agreement with those obtained earlier by Makkonen *et al* [15].

An unexpected result has also been revealed for carbon adsorption at the bridge site (C5) between Pd1 and Pd2 on Pd(320). The adsorbed C atom is found to penetrate the surface spontaneously by pushing the Pd1 atom away from Pd2 and diffusing between Pd1 and Pd2 followed by backward displacement of Pd1 to restore the Pd1–Pd2 bond. As a result, C forms a sub-surface structure in which it has chemical bonds with six neighbouring Pd atoms. The initial and final (equilibrium) geometries of this adsorption are shown in figure 3. This also induces a large outward displacement of Pd1, resulting in a significant (38.1%) increase in $\delta\mathbf{d}_{1,2}$ (see table 2).

3.2. Adsorption energies

For each adsorption site shown in figure 1, we have calculated the adsorption energy E_{ad} for both S and C on Pd(533) and C on Pd(320) and listed them in table 3. We find that, for all sites under consideration, carbon has higher adsorption energy than sulfur. This reflects the difference in the nature of the chemical bonding for S and C, to be discussed in section 3.3. The

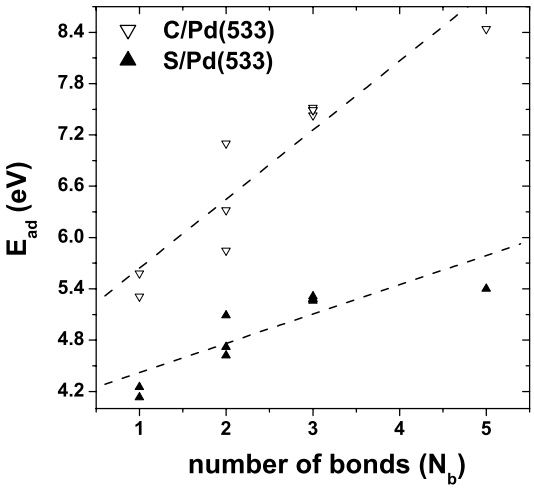

Figure 4. Correlation between C (empty triangles) and S (bold triangles) adsorption energies and the number of adsorbate–Pd bonds extracted from the calculations.

E_{ad} values spread over the range of 4.13–5.40 eV for S and 5.31–8.44 eV for C atoms. Similar is the range of E_{ad} for adsorption on Pd(320) (table 3) for C and [15] for S. As found in earlier work on vicinal surfaces [14, 15], E_{ad} scales roughly linearly with the number of bonds, N_b, that the adsorbate makes with the substrate, as illustrated in figure 4. For Pd(533), the highest E_{ad} is obtained for S or C adsorption at a four-fold hollow site (the site # 1). Then, in the order of decreasing E_{ad} values, we have four three-fold hollow sites (# 2, 3, 4 and 5), three two-fold bridge sites (# 6, 7, and 8) and two on-top sites (# 9 and 10). The physics behind this trend can be understood in terms of the tight binding approximation in which the pC–dPd band width is proportional to the number of nearest neighbours. Broadening the band leads to depopulation of the anti-bonding pC–dPd states, and this way it makes the bonds stronger. Some scattering of the results seen in figure 4 can be attributed to the fact that the notion of the interatomic bond is not well-defined, especially for such complex geometries as those considered in the present work. For instance, formally, carbon adsorbed at the site # 6 has two neighbouring Pds: SC and CC. But, in fact, it also experiences some weak chemical bonding with two BNN atoms. These extra bonds increase the adsorption energy and produce a deviation from the linear dependence. Similarly, C adsorbed at the site # 1 has five bonds: four bonds to the SC and CC Pd atoms which are almost equal, and a fifth bond to BNN which is longer and causes a downward shift of E_{ad}. Nevertheless, the obtained proportionality of E_{ad} to N_b can be used for the rough estimation of adsorption energies of C or S on stepped or kinked Pd surfaces, while deeper insight into the nature of these phenomena can be gained from analysis of the electronic structure.

It is interesting to compare the adsorption energy for C on Pd(533) with those on Pd(211)—two vicinal surfaces with the same terrace geometry but different terrace widths. We find from table 3 here and table I in [14] that the respective adsorption energies are very similar, indicating that the step–step separation on Pd(211) itself is large enough so as to not affect the C binding energy to the Pd atoms.

3.3. Electronic structure

Using the FLAPW method, we have calculated the valence charge densities and local densities of electronic states for Pd(533) and Pd(320) with S and C adsorbed on the site labelled # 1 in

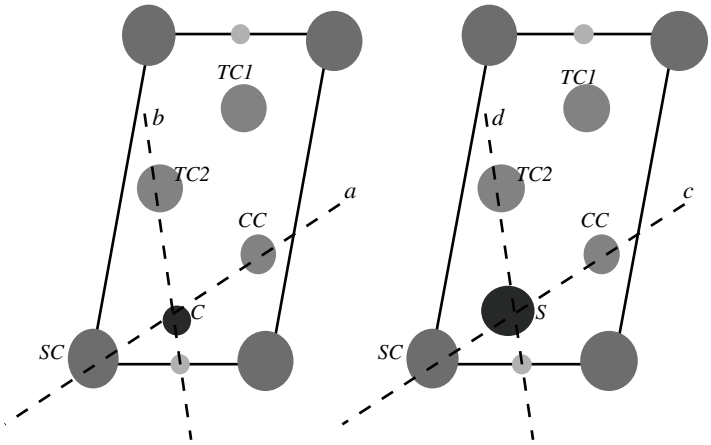

Figure 5. The electronic charge density is plotted along planes a, b, c, and d for Pd(533).

figure 1. To understand the character of chemical bonding between C, S and metal surface atoms, we have plotted the valence charge densities along the planes including the most important C–Pd or S–Pd bonds. Projections of these planes on the (533) surface are shown schematically in figure 5. Note that, as a result of the complex adsorption geometry, the centres of some atoms appear to be slightly out of the planes in the figure. Contour plots of valence charge densities along these planes are shown in figure 6. We cut off high densities around the atomic cores to show in detail the most important low-density charge distribution in interstitial regions. Although in figures 6(a) and (c) the centres of the C and S atoms are not in the plane of interest here, the charge density 'bridges' indicating covalent bonds are clearly seen between the adsorbates and the SC and CC atoms. The densities shown in figures 6(b) and (d) reflect the above-mentioned differences in the locations of C and S on Pd(533): the C atom is linked to BNN, while the S atom is located far from it, but close to the TC2 atom. Further, the intense charge density bridge connecting C and BNN in figure 6(b) suggests strong covalent bonding between these atoms, while, by the same token, the S–TC2 bond appears to be weaker, as seen from figure 6(d).

More details about chemical bonding can be obtained from plots showing the difference $\delta\rho(r)$ between the self-consistent charge density of the system and the sum of densities of free atoms placed at the corresponding sites. Such plots reflect the charge redistribution caused by chemical bonding. Figures 7(a) and (b) show the $\delta\rho(r)$ calculated for C/Pd(533) and S/Pd(533) plotted along the planes (b) and (d) as defined in figure 5. It is seen from the figures that bulk-like Pd atoms (located comparatively far from the surface) donate some electronic density to the interstitial region to build comparatively weak Pd–Pd covalent bonds. Both C and S accept a significant amount of electronic charge from neighbouring Pd atoms, making the C–Pd and S–Pd bonds essentially ionic. However, the distinctive large electronic density bridge between C and BNN atoms (see figure 7(a)) reflects strong C–Pd covalent bonding. In contrast, no significant electronic charge density is seen between S and TC2 atoms in figure 7(b). Thus, the S–Pd bonding in the S/Pd(533) case is mostly ionic with a small covalent contribution, whereas C and the BNN atom form a mixed ionic–covalent bond.

Next we turn to the analysis of the local densities of electronic states (LDOS), which provide additional information about the character of chemical bonding between adsorbates and metal atoms and some insights about properties related to catalytic activity of the surfaces. In figure 8 we show LDOS calculated for S/Pd(533) and C/Pd(533). We find a large splitting

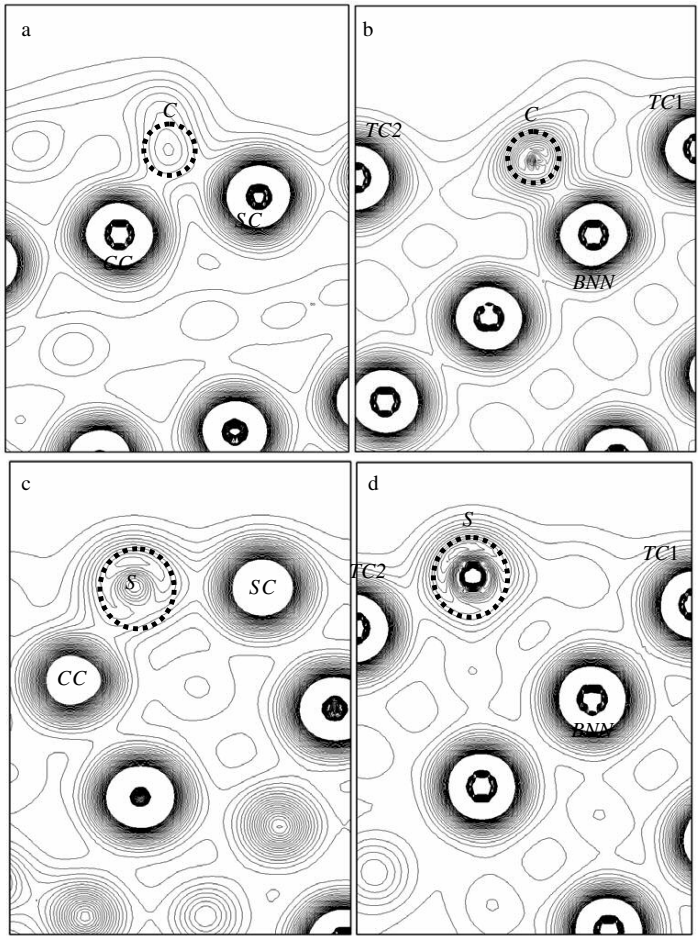

Figure 6. Valence electronic density calculated for (a) $C_{0.25}$/Pd(533) at adsorption site 1 and plotted along plane *a* in figure 5 normal to the surface and including C, TC1, TC2, and BNN atoms, (b) $C_{0.25}$/Pd(533) along plane *b* in figure 5 including SC, CC and C atoms, (c) $S_{0.25}$/Pd(533) at adsorption site 1 and along plane *c* in figure 5 including SC, CC and S atoms, and (d) along plane *d* in figure 5 including S, TC1, TC2, and BNN.

of p states of C and S with two main structures (A and B in the figure) separated by (7–8 eV). Since similar (but less intense) structures are found in the LDOS of Pd atoms at the same energies, we conclude that there is a strong hybridization of adsorbate p states with the local states of surface Pd atoms. The B and A structures thus represent bonding and anti-bonding states, respectively. As seen from the figure, the SC, CC and BNN surface atoms are involved in the hybridization. The B and A structures in the LDOS of carbon are quite distinct (low density between them) and the anti-bonding states are empty. These are indications of strong covalent C–Pd bonding, in agreement with the obtained valence charge densities. In contrast, only part of the p states of sulfur is involved in the hybridization (the rest are distributed between B and A structures). Furthermore, the S anti-bonding states are partially occupied. This explains why the S–Pd covalent bonds are weak, as inferred also from the plots of the valence charge densities in figure 8.

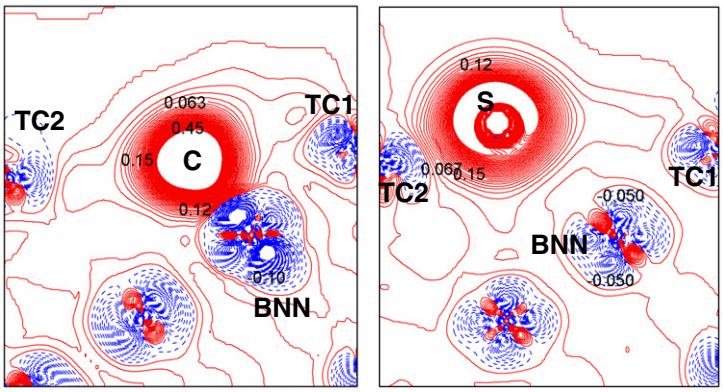

Figure 7. Valence electronic density redistribution in $C_{0.25}$/Pd(533) (on the left) and $S_{0.25}$/Pd(533) (on the right) with respect to the sum of densities of noninteracting atoms. Solid (red) and dashed (blue) lines denote the positive and negative deviation, respectively.

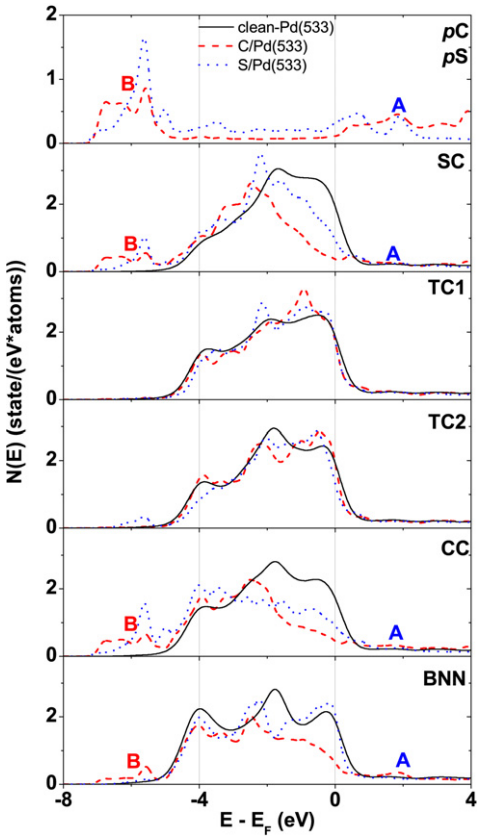

Figure 8. Local density of C, S and Pd electronic states calculated for $C_{0.25}$/Pd(533) with adsorption site 1 (dashed red line), $S_{0.25}$/Pd(533) at site 1 (dotted blue line) and for clean Pd(533) (solid black line).

Similar results are obtained for the adsorbates on Pd(320) (see figure 9): there is a strong hybridization between the electronic states of the adsorbate and neighbouring Pd atoms, and

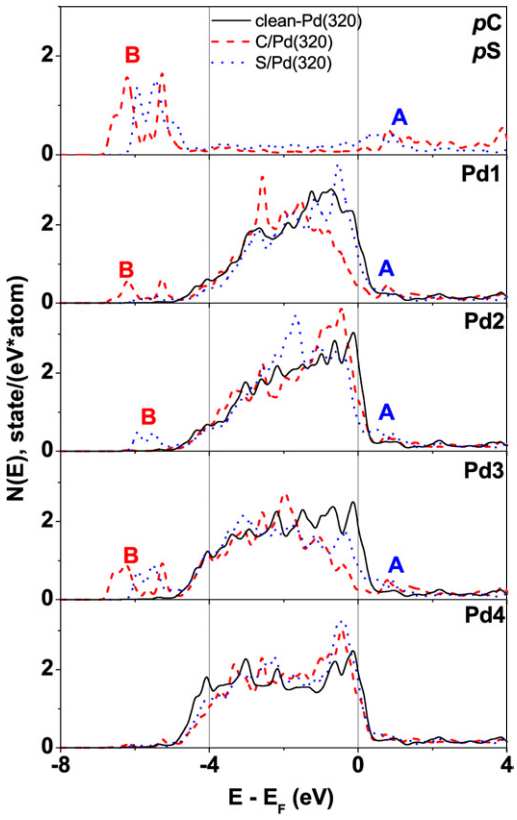

Figure 9. Local density of C, S and Pd electronic states calculated for $C_{0.33}$/Pd(320) with adsorption site 1 (dashed red line), $S_{0.33}$/Pd(320) at site 1 (dotted blue line) and for clean Pd(320) (solid black line).

Table 4. Local density of states at Fermi level (state/eV $*$ atoms) calculated for Pd surface atoms in clean Pd(533), S/Pd(533), and C/Pd(533).

	SC	TC1	TC2	CC	BNN
Clean-Pd(533)	2.01	1.95	2.00	1.78	1.93
S/Pd(533)	0.93	1.73	1.30	0.90	2.04
C/Pd(533)	0.37	1.78	1.98	0.46	0.65

because of larger B–A splitting and fewer occupations of the anti-bonding states, carbon forms stronger covalent bonds with Pd than by sulfur.

Such significant modification of the electronic structure as have documented above for the Pd surfaces upon C and S adsorption should affect their properties. Since Pd is a widely used catalyst, the property of interest is its catalytic activity (reactivity). Recalling the model that links the surface reactivity to the local density of electronic states at the Fermi level $[N_a(E_F)]$ [13], we examine the change in this quantity upon C and S adsorption on the Pd surfaces. As seen from figures 8 and 9, the splitting caused by hybridization reduces the LDOS around the Fermi level dramatically for Pd atoms, which have direct covalent bonds with the adsorbate. In tables 4 and 5 we list $N_{Pd}(E_F)$ calculated for clean Pd(533) and Pd(320), as well as for those adsorbed with C and S. All atoms of the clean Pd surfaces are found to have a high

Table 5. Local density of states at Fermi level (states/eV $*$ atoms) calculated for Pd surface atoms in clean-Pd(320), S/Pd(320), and C/Pd(320).

	Pd1	Pd2	Pd3	Pd4
Clean-Pd(320)	1.59	2.26	1.81	1.88
S/Pd(320)	1.13	0.73	0.83	1.63
C/Pd(320)	0.44	1.27	0.24	1.30

$N_{\mathrm{Pd}}(E_{\mathrm{F}})$, which are not much affected by the presence of the step or kink. This is consistent with the fact that Pd is an efficient catalyst. For both Pd(533) and Pd(320), the presence of C and S leads to a drastic decrease in $N_{\mathrm{Pd}}(E_{\mathrm{F}})$ for neighbouring Pd atoms, while the next neighbours are only slightly affected. Thus we can expect that both S and C poison the surface reactivity of Pd(533) and Pd(320). Interestingly, for the case of S/Pd(533), the $N_{\mathrm{Pd}}(E_{\mathrm{F}})$ are suppressed for SC, TC2 and CC, which are all exposed to the surface. On the other hand, for C/Pd(533), three Pd sites (SC, CC and BNN) are strongly affected, but only two of them (SC and CC) are exposed to the surface. Since only actual surface atoms are involved in catalytic reactions, a decrease in the $N_a(E_{\mathrm{F}})$ of BNN should not affect the surface reactivity. Nevertheless, the effect of C on the $N_{\mathrm{Pd}}(E_{\mathrm{F}})$ of Pd(533) is remarkable. Again, the effect of the S and C adsorbates on the $N_{\mathrm{Pd}}(E_{\mathrm{F}})$ of metal atoms in Pd(533) appears to be similar to that obtained earlier [14] for Pd(211). However, in the case of Pd(211), this results in the suppression of $N_{\mathrm{Pd}}(E_{\mathrm{F}})$ for all surface atoms, while in Pd(533), which has wider terrace, some surface atoms continue to retain high values of $N_{\mathrm{Pd}}(E_{\mathrm{F}})$.

4. Conclusions

In the present work we have studied from first principles the effect of adsorption of carbon and sulfur on the geometric and electronic structures of the stepped surfaces Pd(533) and Pd(320). We find the surface lattice to be perturbed dramatically in response to the adsorption. Our calculations show that C adsorbed at the bridge site at the edge of the Pd chain in Pd(320) penetrates the surface to form a sub-surface structure. The adsorption energies are found to be site dependent, ranging from 5.31 to 8.58 eV for C and from 2.89 to 5.40 for S. The S–Pd and C–Pd bondings have mixed ionic–covalent character, with prevailing covalency for the C–Pd bonds and dominating ionicity for the S–Pd bonds. The strong hybridization between adsorbate and metal electronic states results in a large splitting of the bands, which causes a dramatic suppression of the local densities of states at the Fermi level for Pd surface atoms neighbouring the adsorbate. This effect is expected to poison the catalytic activity of these surfaces. We have compared the results obtained for C and S chemisorption on Pd(533) with those obtained earlier for Pd(211) [14]. These two stepped surfaces have similar structures, but Pd(533) has a terrace that is wider by one atomic chain. The adsorption energies, surface relaxation patterns and the effects of adsorbates on the local densities of electronic states and valence charge densities obtained for both surfaces are found to be quite similar, suggesting the local character of the adsorbate impact on geometric and electronic structures of Pd surfaces.

Acknowledgments

This work was supported by the US Department of Energy under grant no. DE-FGO3-03ER15445. We thank H Freund and G Ruprechter for helpful discussions.

References

[1] Hammer B and Nørskov J K 1997 *Phys. Rev. Lett.* **79** 4441
[2] Gambardella P, Zljivancanin Z, Hammer B, Blanc M, Kuhnke K and Kern K 2001 *Phys. Rev. Lett.* **87** 056103
[3] Dahl S, Logadottir A, Egeberg R C, Larsen J H, Chorkendorff I, Törnqvist E and Nørskov J K 1999 *Phys. Rev. Lett.* **83** 1814
[4] Feibelman P J, Esch S and Michely T 1996 *Phys. Rev. Lett.* **77** 2257
[5] Hammer B 1999 *Phys. Rev. Lett.* **83** 3681
[6] Hammer B 2001 *J. Catal.* **199** 171
[7] Mavrikakis M, Stoltze P and Nørskov J K 2000 *Catal. Lett.* **64** 101
[8] Loffreda D, Simon D and Sautet P 2003 *J. Catal.* **213** 211
[9] Savio L, Vattuone L and Rocca M 2001 *Phys. Rev. Lett.* **87** 276101
[10] Xu J and Yater J T 1993 *J. Chem. Phys.* **99** 725
[11] Liu Z-P and Hu P 2004 *Top. Catal.* **28** 71
[12] Liu Z-P and Hu P 2003 *J. Am. Chem. Soc.* **125** 1958
[13] Feibelman P J and Hamann D R 1984 *Phys. Rev. Lett.* **52** 61
[14] Stolbov S, Mehmood F, Rahman T S, Alatalo M, Makkonen I and Salo P 2004 *Phys. Rev.* B **70** 155410
[15] Makkonen I, Salo P, Alatalo M and Rahman T S 2003 *Phys. Rev.* B **67** 165415
[16] Wilke S and Scheffler M 1996 *Phys. Rev. Lett.* **76** 3380
[17] Rose M K, Borg A, Mitsui T, Ogletree D F and Salmeron M 2001 *J. Chem. Phys.* **115** 10927
[18] Rutkowski M, Wetzig D and Zacharias H 2001 *Phys. Rev. Lett.* **87** 246101
[19] Habermehl-C'wirzen' K and Lahtinen J 2004 *Surf. Sci.* **573** 183
[20] Bowker M and Morgan C 2004 *Catal. Lett.* **98** 67
[21] Kohn W and Sham L 1965 *Phys. Rev.* **140** A1133
[22] Perdew J P and Wang Y 1992 *Phys. Rev.* B **45** 13244
[23] Payne M C, Teter M P, Allan D C, Arias T A and Joannopoulos J D 1992 *Rev. Mod. Phys.* **64** 1045
[24] Vanderbilt D 1990 *Phys. Rev.* B **41** 7892
[25] Weinert M, Wimmer E and Freeman A J 1982 *Phys. Rev.* B **26** 4571
Singh D 1994 Planewaves *Pseudopotentials and the LAPW Method* (Dordrecht: Kluwer)
[26] Blaha P, Schwarz K, Madsen G K H, Kvasnicka D and Luitz J 2001 *WIEN2K, An Augmented Plane Wave + Local Orbitals Program for Calculating Crystal Properties* Karlheinz Schwarz, Technische Universität Wien, Austria
[27] Monkhorst H J and Pack J D 1976 *Phys. Rev.* B **13** 5188
[28] *American Institute of Physics Handbook* 1970 (New York: McGraw-Hill) Table 9a-2
[29] Pussi K, Hirsimäki M, Valden M and Lindroos M 2004 *Surf. Sci.* **566–568** 24